Submitted to CDMG Coalinga Volume
September 1983

REVERSE SLIP ON A BURIED FAULT DURING THE 2 MAY 1983 COALINGA EARTHQUAKE: EVIDENCE FROM GEODETIC ELEVATION CHANGES

by

Ross S. Stein[1]

ABSTRACT

The Coalinga Earthquake (M_L=6.2-6.7) uplifted Anticline Ridge one half meter, but caused no fault rupture at the ground surface, demonstrating that folding and faulting of the eastern margin of the California Coast Ranges are coincident and continuing. Elevation changes associated with the earthquake enable an estimate of the fault attitude, geometry, and slip. Small topographic relief over the route minimizes systematic leveling errors. Artificial subsidence due to fluid withdrawal is more significant, although it is still small in relation to the earthquake changes. Deep-well compaction monitors and the record of fluid pumping are used to remove the subsidence. A steeply-dipping reverse fault is well fit by the geodetic and seismic data, whereas a gently-dipping thrust fault is less compatible with the location and depth of the mainshock. For a N53°W strike and a 67°NE dip, the best-fit earthquake parameters are: 1.8±0.5 m of dominantly reverse dip slip on a fault extending from a depth of 10-13 km to within 3-5 km from the ground; M_o = 6-7 x 10^{25} dyne-cm. The deformation caused by the 1983 earthquake looks strikingly like the present-day topographic form of Anticline Ridge. About 2-5 km of cumulative buried fault slip during the last million years would account for this similarity.

INTRODUCTION

The 2 May 1983 Coalinga earthquake struck beneath Anticline Ridge, at the boundary of the San Joaquin Valley syncline to the east, and the California Coast Ranges to the west. The tectonic role of the earthquake - its repeat time and the cumulative displacement on the earthquake fault - and its impact upon strain accumulation on the San Andreas fault 30 km to the west, cannot be interpreted without knowledge of the fault attitude and amount of slip. The range of fault geometries and displacements consistent with the permanent vertical deformation and earthquake mainshock are presented in this paper.

Spirit leveling measures the height of permanent bench marks (BM's) in the ground. To obtain changes in elevation caused by the earthquake, the elevation of BM's surveyed largely 11 years before the earthquake is subtracted from the elevation measured one month after the 2 May 1983 earthquake. While random and systematic leveling errors prove to be negligible in comparison to the magnitude of the earthquake deformation, artificial subsidence caused by water- and oil-withdrawal is more substantial. Uncertainties in the proper removal of these contaminants limit the ability to model the earthquake.

The earthquake rupture is modeled with dislocations embedded in an elastic half-space. This is equivalent to making a rectangular cut within an elastic body, displacing the faces of the cut a prescribed amount, and gluing them

[1]U.S. Geological Survey, Menlo Park, California 94025

back together. The surface of the elastic body will be deformed, and this deformation is matched to the observed data. Dislocation models are non-unique: Here they are kept as simple as possible, limited by the constraints imposed by the mainshock fault plane solution. Because the leveling route is oriented across the geologic structure and passes near the mainshock epicenter, the pattern of surface deformation allows the fault plane to be distinguished with fair confidence from the auxilliary plane. Subject to a poorly constrained fault length along strike, the seismic moment (M_0) can be estimated for comparison with the moment measured from seismic waves; M_0 is proportional to the slip times the fault area. The fault slip and the depths to the top and base of the fault are important to distinguish faulting from the regime above the fault where folding predominated during the earthquake.

DATA

The 2 May 1983 Coalinga earthquake struck within a leveling network established to study compaction of unconsolidated deposits in responce to ground-water withdrawal [Bull, 1975]. The 50 km-long network of leveling routes (Figure 1) was surveyed in 1960, 1966, 1969, and 1972 by the National Geodetic Survey (NGS) for the U.S. Geological Survey (USGS). The NGS releveled the net during 8-24 June 1983 at the request of the USGS. The network is ideally located to study earthquake elevation changes, but suffers from bench mark subsidence caused by ground-water withdrawal in Pleasant Valley and the San Joaquin Valley, and by oil withdrawal beneath Anticline Ridge (Figure 1). Subsidence is evident on the 1966-1972 profile of elevation change before the earthquake occured (Figure 2a).

Leveling Errors

Sources of measurement uncertainty in leveling are dominated by slope-dependent systematic errors. These include improper calibration of the graduated leveling rods, and atmospheric refraction of the line of sight between the rods and the level, a horizontal telescope. Typical errors in the length of leveling rods used during the period 1953-1979 are less than 25 ppm at the 95% level of confidence [Strange, 1980; Stein, 1981]. Because the maximum elevation difference encountered on the leveling route is 200 m (see Figure 2d), rod errors of 5 mm are possible. Elevation changes shown in Figure 2 have been corrected for refraction error using the method of Holdahl [1981]. Most of the refraction error that accumulated along a 50 km-long test route in southern California was removed by this method, using similar procedures and under climatic conditions similar to those that prevail in Coalinga, [Holdahl, 1982; Stein et al., in prep.]. Residual refraction error should be less than 5 mm, assuming a 100% error in estimating the mean temperature gradient along the line of sight and a 50% error in estimating the mean distance between the level and rods for the 1972 survey. Random errors grow with the square root of the distance leveled. Because all of the leveling reported here was performed to first-order double-run standards [Federal Geodetic Control Committee, 1980], the random error should accumulate to less than 10 mm over the 35 km distance between the southwest and northeast ends of the route. Leveling errors from all sources thus sum to less than 20 mm, equal to the size of the bench mark symbols in Figure 2.

EARTHQUAKE ELEVATION CHANGES

The 1966-72 subsidence rate is employed to remove artificial subsidence that took place after 1972, modified by the record of surficial compaction and fluid extraction during 1972-83. Bench marks in consolidated Cretaceous rocks (F1046-J944, Figure 1; BM's 1-6, Figure 2a) are assumed to be stable during the preseismic 1966-72 period. These bench marks are also farthest from the sites of known artificial subsidence. During the 1972-83 earthquake period, this assumption is no longer tenable; no bench mark is more than 20 km from the mainshock epicenter. Therefore the position of the zero elevation change datum in Figures 2b and 2c (the thin horizontal line) is arbitrary.

San Joaquin Valley Subsidence

Subsidence caused by artesian head decline along the western margin of the San Joaquin Valley reached a peak during the mid-1950's, and largely abated after construction of the California aqueduct replaced deep aquifer pumping [Bull, 1975]. During the period 1970-1980, the aqueduct delivered 93% of the total water used for irrigation [Ireland et al., 1982]. Because of the reduced rate of head decline after 1970, the rate of subsidence during 1966-72 (Figure 2a) provides an upper bound on the rate for the ensuing decade.

Poland, et al. [1975] and Bull [1975] report on deep well compaction recorders that measure the vertical strain or shortening caused by compaction of surface deposits and the heavily pumped aquifers. Compaction well 33A1, 313 m deep, is located at the northeast end of the main leveling route (marked by an X in Figure 1a). From March 1966, a year after its installation, through January 1980, the end of the published record, the well recorded 275 mm of compaction [Ireland et al., 1982]. The California Department of Water Resources releveled the route from BM Y998 USGS, adjacent to the recorder well, to BM E929 atop Anticline Ridge in February 1982 (the BM's are shown as circles in Figure 1a; BM's 27-37 in Figure 2a). Subsidence of BM Y998 USGS from March 1966 to February 1982 was 300 mm. Therefore the compaction recorder measured at least 90% of the total subsidence. The rate of compaction during the period 1972-1980 is 30% of the 1966-72 rate, suggesting that the subsidence rate also decreased by about 30%. Compaction well 23P2, 670 m deep, operated though 1974 (X at end of east spur marked by triangles in Figure 1a). During 1966-72 the well recorded 100% of the subsidence at nearby BM Z888. During the succeeding two years the rate of compaction was 40% of the rate during 1966-72. Under the assumption that the aquifer continued to recharge after 1974, the projected 1972-83 subsidence rate would be about 30% of the 1966-72 rate.

The compaction history of wells with recorders therefore suggests that the elevation of bench marks surveyed during 1972 should be corrected for subsidence at a rate equal to 30% of the 1966-72 rate. Bench marks in recent alluvium (east of the subsidence boundary in Figure 1b) have been corrected for subsidence in Figure 2c. Probable error in the correction should be less than 50% of the estimated 1972-83 subsidence rate, or 45 mm at the end of the north spur where the 1972-83 subsidence rate is estimated to be 8 mm/yr (squares in Figure 1; BM E927), 55 mm at the end of the east spur where the rate is 10 mm/yr (triangles; BM H927), and only a few mm at the end of the main route where the 1982-83 rate of subsidence is 6 mm/yr (circles in Figure 1; BM Q1195).

Pleasant Valley Subsidence

The rate of subsidence in Pleasant Valley during 1960-72 was about one third of the rate in the San Joaquin Valley [Propokovitch and Magleby, 1968], but subsidence in Pleasant Valley after 1972 is more uncertain because no wells record compaction there, and because no releveling was conducted there during 1972-82. Aqueduct deliveries to the Coalinga township during 1972-82 comprised 30% of the total water consumption, whereas the aqueduct supplied only 2% of the water during 1970-71 [unpub. Bureau of Reclamation Water Delivery Records for 1983]. Estimated groundwater pumpage (for Township/Range 20S/15E) decreased by 40% from 1966-71 to 1975-77 [Mitten, 1972, 1976, 1980]. No pumping records are available for the years 1972-74 and 1978-83, but continued water table decline increased the cost of pumping for irrigation; this probably reduced pumpage after 1977. Here it is assumed that the subsidence rate during the period 1972-83 was about 50% of the rate during 1966-72. The maximum 1972-83 subsidence rate in the Valley, at BM's 12 and 17 in Figure 2b, becomes 9 mm/yr - roughly equivalent to the rate in the San Joaquin Valley - with an uncertainty of perhaps 4 mm/yr, or 45 mm.

Anticline Ridge Subsidence

The net liquid production rate beneath Anticline Ridge has remained unchanged since 1966, at 34 million bbl/yr [5.4 million m^3/yr; Conservation Committee of California Oil Producers, 1967-1982]. This includes the combined pumping of oil and water, minus re-injected water and steam, in the Coalinga and East Extension fields that are traversed by the leveling route. The 1966-72 subsidence rate is therefore employed to correct the earthquake elevation changes of BM's W944 - U237 and J929 - Y156 in Figure 1a (BM's 22-26 and 46-49 in Figure 2a). North of the oil fields and south of the recent alluvium, BM's Y662 - X662 showed no subsidence during 1960-72 (Figure 1; BM's 37-42, Figure 2a); therefore no corrections were made to these BM's in Figure 2c.

To summarize, subsidence corrections are generally small in comparison to the total observed elevation changes during the earthquake period; corrections nowhere exceed 110 mm. The largest corrections are made to the main leveling route in Pleasant Valley, and to the north and east spurs in the San Joaquin Valley. The portion of the main route in the San Joaquin Valley was leveled only 1.5 yrs before the earthquake, and therefore sustained little artificial subsidence.

DISLOCATION MODELS

The earthquake elevation changes are modeled by dislocations in an elastic half-space using expressions of Mansinha and Smylie [1971] and with Poisson's ratio, the ratio of contraction of a body in one direction to the amount it is stretched in the perpendicular direction, set to 1/4. The half-space is a body with infinite depth and with a flat upper surface approximating the ground. A fault is modeled by a rectangular plane with uniform slip on its surface. Faults in the earth are not rectangular, not planar, and can not maintain uniform slip on their surfaces without producing infinite stress changes at their perimeters. However, these simplifications do not modify the vertical deformation at the ground surface enough to warrant the use of other more plausible geometries.

Testing of candidate fault models was simplified by adherence to the fault plane solution of Eaton [1983] from first motion of P-wave polarities at 39 stations less than 100 km from the epicenter. The model fault strike was therefore fixed to be N53°W. A N37°E+20° axis of maximum compression suggests reverse dip slip. This means that up to a 20° right-lateral or left-lateral slip component is permissible. With one exception, model faults were constrained to pass within 1.5 km of the mainshock hypocenter, which is located at 36°13.99'N latitude, 120°17.59'W longitude, at a depth of 10.5 km. One nodal plane dips 67°NE, and the other dips approximately 23°SW. Model faults are shown with aftershocks $M_L \geq 3$ within the first four days of the 2 May earthquake [Reasenberg et al., 1983]. In the absence of primary ground surface rupture [Clark et al, 1983; Hart and McJunkin, this volume], both planes were tested.

Northeast-Dipping Reverse Fault

The general characteristics of the earthquake deformation limit choices for the fault location and geometry. For a reverse fault plane, the peak ground uplift occurs above the upper edge or top of the fault, and the elevation change is zero where the fault plane would intersect the ground if extended to the surface (See Figure 3a). For a fixed dip and depth to the center of the fault, the product of the slip times the fault width (the down-dip fault dimension) is shared by all acceptable models. The fault length is poorly guaged by the data, since the leveling is not extensive along strike and the aftershocks are distributed over a very large area. A fault length of 14-16 km appears consistent with the decay of elevation change at the northern and eastern ends of the leveling network (squares and triangles in Figure 1a). Thus for all successful models with pure reverse slip, M_o = 6.0-6.5 $\times 10^{25}$ dyne-cm (6.0-6.5 $\times 10^{18}$ Nm), where $M_o = G \cdot U \cdot A$, G is the shear modulus, here assumed to be about 3×10^{11} dyne/cm^2 (3×10^{10} N/m^2), U is the slip, and A is the fault area.

For a 67°NE dip, the vertical depth to the top of the fault (the depth of burial of the fault's upper edge) is equal to about two thirds the width of the peak-to-trough elevation change. The uncertainty in the depth of burial stems from inconsistent elevation changes and uncertain artificial subsidence of BM's near Coalinga, 10 km southwest of the epicenter. To simplify the presentation of the three models shown in Figure 3a, the fit to the eastern spur (triangles) is not shown. The surface projection of the fault models represented by a dotted line and by a dashed line in Figure 3a is shown in Figure 1b. The geodetic data can permit up to 20° of right-lateral or left-lateral slip on the steeply dipping reverse fault with a slight increase in M_o (Figure 3b). A left-lateral component of slip is more easily fit to the leveling data; right-lateral slip cannot be imposed unless the southeastern edge of the fault lies with a few km of the mainshock epicenter.

Southwest-Dipping Thrust Fault

The peak uplift along the leveling route occurs near the mainshock epicenter. Because the uplift must locate above the top of the fault, the upper edge of a gently dipping model fault must pass through the mainshock hypocenter. Thus the upper edge of the fault must lie at a depth of about 10 km (the dot-dash line in Figure 3c). The deeply buried fault requires more slip

to uplift the ground surface the same amount as faults at shallower depths; thus for a fault length of 14 km, M_0 = 9 x10^{25} dyne-cm. A mainshock at the upper edge of a fault also implies seismic rupture in the down-dip direction. The fit to the observed elevation changes is poor.

A good fit to the observations using a southwest-dipping thrust plane can be accomplished with more complex models. A thrust fault situated 6 km above Eaton's [1983] hypocentral depth with fault slip increasing down-dip provides an excellent fit to the leveling data (dotted line in figure 3c). However, the mainshock would not locate on the fault plane unless its epicenter were relocated 6.5 km to the southwest and its depth were reduced from 10.5 km to 7.5 km. In order to satisfy the condition that the model fault should pass through the mainshock, a curved fault surface or one in which the fault dip increases above the hypocenter becomes necessary (Figure 3d). The steeply dipping segment with 1 m of aseismic reverse slip brings the predicted elevation change at the northeast end of the leveling route into better agreement with the data. Some misfit remains in the region from the epicenter extending for 10 km to the southwest. The surface projection of this fault model is shown by a solid line in Figure 1b. The parameters of all the fault models shown in Figure 3 are presented in Table 1.

Table 1: Fault Models

Strike/Dip	Slip Direction[1]	Slip m	Vertical Depth To: Top of Fault km	Base of Fault km	Fault Width km	Moment[2] M_0x10^{25} dyne-cm	Model Fit	Fig. 3 Symbol
N53°W67°NE	reverse	1.3	3.0	13.2	11.0	6.5	good	a - - -
N53°W67°NE	reverse	1.8	4.0	11.2	8.0	6.0	good	a ———
N53°W67°NE	reverse	2.3	5.0	10.5	6.0	6.0	good	a ·····
N53°W67°NE	reverse w/ 20°rt-lat.	2.2	4.5	11.0	7.0	6.5	good	b ·····
N53°W67°NE	reverse w/ 15°lft-lat.	1.8	4.0	11.5	8.0	7.0	good	b ———
N53°W23°SW	thrust	2.5	10.5	13.2	10.0	9.0	poor	c —·—
N53°W23°SW	thrust	1.4, top 2.0, base	4.5	7.2	9.0	5.0	good[3]	c ·····
N53°W60°SW N53°W23°SW	reverse thrust	1.0, top 2.0, base	5.0	12.0	11.0	7.5	fair	d ———

Notes: 1/Strike, Dip, and Slip Direction are constrained by Eaton's [1983] fault plane solution for the 2 May 1983 Mainshock. 2/Fault length along strike is not well constrained; 14-16 km is used. 3/Fault lies 6 km above the mainshock hypocenter.

INTERPRETATION

Steeply-dipping Reverse Fault or Gently-dipping Thrust?

The earthquake elevation changes are well fit by a northeast-dipping thrust fault extending from a depth of 3-5 km to 10-13 km, with 1.3-2.3 m of reverse dip slip. A southwest-dipping thrust plane can fit the data equally well if it is sufficiently shallow, and if the fault slip increases down-dip. However, the depth of seismicity argues against the likelihood that such a shallow thrust fault produced the earthquake elevation changes. Both the mainshock and the larger immediate aftershocks in the epicentral area lie beneath the 4-7 km depth of the candidate thrust fault (Figure 3c). While these hypocenters are preliminary, the presence of a seismic station 5 km northwest of the mainshock renders location and depth changes of 5 km unlikely [Reasenberg et al., 1983]. The earthquake could have ruptured the curved or two-plane thrust fault shown in Figure 3d, but the fit to the leveling data is inferior to the reverse fault models. The uncertainty of bench mark subsidence in Pleasant Valley does not permit rejection of the two-plane model. The apparent absence of seismic radiation from the steeply-dipping upper portion of such a fault could be explained by seismic rupture from 10-14 km in the down-dip direction, preceeded or followed by aseismic slip from a depth of 5-10 km. Barring significant relocation of the mainshock and after shocks, though, the steeply dipping reverse plane provides the most straightforward fit to the geodetic and seismic evidence. Wentworth et al [this volume] find evidence from seismic refraction and reflection data for both a steeply-dipping reverse fault and a gently-dipping thrust fault beneath the southern end of the Kettleman Hills anticline, a similar structure 65 km south of Coalinga.

The seismic moment for the successful fault models was found to be in the range 6-7 $\times 10^{25}$ dyne-cm (6-7 $\times 10^{18}$ Nm). The moment could be larger if the fault plane extended further to the northwest or southeast along strike, but it is unlikely to be much smaller. Heaton and Hartzell [this volume] calculate $M_0 = 3.8 \times 10^{25}$ dyne-cm from teleseismic long period (5 sec) compressional waves; Kanamori [this volume] determines $M_0 = 5.4 \times 10^{25}$ dyne-cm from very long period (250 sec) surface waves. Unless the fault length proves to be much longer than 15 km, the fair agreement between geodetic and seismic estimates of M_0 implies that most slip was released seismically during the mainshock.

Folding of Anticline Ridge

The modeling demonstrates that most of the earthquake fault slip was confined to depths greater than 3-5 km. If fault slip tapered from a depth of 5 to 3 km, the vertical deformation would look similar to that if rupture terminated at 4 km. Similarly, if slip was distributed over a fault thickness of 1 km rather than confined to a plane, the dislocation models would overestimate the upper fault depth. Thus the depth of burial values should be considered maximum estimates. Particularly at the ends of the fault where no deformation data exists, some slip could penetrate closer to the ground surface. It is thus stiking that a number of the deepest wells in the oil fields [California Division of Oil and Gas, 1973] above the probable fault appear properly located to have sustained some primary fault rupture (Figure 1b).

Whereas elastic strains are relieved in rocks near the seismic fault at depth, the earthquake increased strains in the rocks that lie between the top of the fault and the ground surface. If earthquakes do not periodically rupture through to the surface, then the strains must be relaxed by creep. The near-absence of aftershocks at depths above 4-5 km in the epicentral region, where a great thickness of unconsolidated Pleistocence sediments have folded into an anticline, suggests that these rocks are too weak to accumulate and maintain high stresses: They do not fail seismically but fold instead. This speculation finds support in the absence of a fault scarp at the base of Anticline Ridge in the Tertiary and younger rocks (Figure 1a). If during the Pleistocene numerous earthquakes occured with magnitudes similar to the 1983 shock, such a scarp would be produced. In contrast to the seismic behavior of the Tertiary section, very shallow aftershocks occured in the Cretaceous section northwest of Pleasant Valley [Figure 1a; also see Reasenberg et al, 1983]. On 9 May 1983, a M_L=5.2 aftershock at a depth of 3.4 km produced a 4 km-long surface rupture with 0.6 m of reverse dip slip [Hart and McJunkin, this volume]. The M_L=7.2 1952 Kern County earthquake - also a steeply-dipping reverse fault - exhibited similar behavior. The fault ruptured the surface in Cretaceous granites, but failed to penetrate the upper 5 km of the Pliocene and Pleistocene sediments of Wheeler Ridge anticline at the earthquake epicenter [Stein and Thatcher, 1981]. King and Brewer [1981] found that near-surface folding also accompanied reverse fault slip during the Ms=7.3 1980 El Assam earthquake.

Cumulative Reverse Fault Slip During the Pleistocene

The striking similarity between the form of the earthquake deformation and the topographic profile can be seen by inspection of Figures 2c and 2d. The topographic form of the Ridge also conforms to the subsurface structure (Figure 1a). Although folding of the anticline commenced in the late Eocene (40 million years ago), the rate of deformation increased during middle Pleistocene time (less than one million yrs ago): Exposed Pleistocene beds dip 20-40° on the limbs of the anticline [Harding, 1976] where the topographic slope is about 5°. The amplitude of the fold may thus be as much as four times greater than the amplitude of the topography, because erosion from highs and deposition into lows diminish the topographic gradient. In fact the topography could be created by repeated earthquakes if the fault did not often rupture to the surface. Geodetic tilt in Figure 2c is correlated with the topographic slope in Figure 2d at the 99% level of confidence; the mean slope is equal to 800 + 150 times the tilt [for the details of the correlation method, see Stein, 1981]. Because slope-dependent leveling errors cannot attain this magnitude, the correlation must reflect the growth of the fold. Since slip during the 1983 Coalinga earthquake was found to be 1.8 + 0.5 m, a cumulative displacement of 2-5 km on the fault at depths below 4 km would build the present-day topography. King and Stein [this volume] suggest an approximate repeat time for earthquakes at Coalinga of 350 yrs, on the basis of uplifted and distorted river terraces formed where creeks draining the eastern Coast Ranges cut through the anticlinal axes into the San Joaquin Valley (see Figure 1a). If the fault slipped mostly during earthquakes similar in size to the 1983 event, then 2-5 km of reverse slip may have accumulated at depth during the last 350,000 - 1 million yrs.

CONCLUSION

The 2 May 1983 Coalinga earthquake most probably ruptured a fault that dips steeply to the northeast beneath Anticline Ridge. Reverse dip slip of 1.8 ± 1.5 m from a depth of 4±1 km to the hypocenter at 11.5 ± 1.5 km provides the fit most compatible with the geodetic and seismic data. A thrust fault dipping gently to the southwest is not precluded by the geodetic data, but the fit to both leveling and seismic data is less satisfactory than for the reverse fault. Folding of Anticline Ridge appears to accompany buried reverse faulting, most likely because the poorly lithified sediments are too weak to store significant elastic strain, and creep instead. This hypothesis would explain both the absence of 1983 surface breakage at the base of Anticline Ridge, and the lack of shallow aftershocks in the epicentral region. In contrast to this, both ground rupture and large shallow aftershocks are evident during the 1983 Coalinga sequence in the Cretaceous rocks northeast of Anticline Ridge. The similarity between the topographic form of Anticline Ridge and the earthquake elevation changes is compelling enough to extrapolate 2-5 km of cumulative buried fault slip during the last million years.

ACKNOWLEDGEMENTS

The author is indebted to E. Balazs and B. Martine of the National Geodetic Survey for rapidly surveying the leveling network. Exciting discussions with A. Lindh, G. King, and C. Wentworth contibuted to this effort. W. Thacther, D. Oppenheimer, and D. Eberhart-Phillips reviewed the manuscript.

REFERENCES

Bull, W. B., 1975, Land subsidence due to ground-water withdrawl in the Los Banos-Kettleman City area, California. Part 2, Subsidence and compaction of deposits: U.S. Geol. Survey Prof. Paper 437-F, 91 p.

California Division of Oil and Gas, 1973, North and east central California, Data sheets and Index maps: California Division of Oil and Gas, V.1, 22 p.

Clark, M., Harms, K., Lienkaemper, J., Perkins, J., Rymer, M., and Sharp, R., 1983, The search for surface faulting, in Borcherdt, R. D., ed., The Coalinga earthquake sequence commencing May 2, 1983: U.S. Geol. Survey open-file report 83-511, 79 p.

Conservation Committee of California Oil Producers, 1982 and earlier, Annual review of California oil and gas production: Conservation Committee of California Oil producers, annual production statistics.

Eaton, J., 1983, Seismic setting, location, and focal mechanism, in Borcherdt, R. D., ed., The Coalinga earthquake sequence commencing May 2, 1983: U.S. Geol. Survey open-file report 83-511, 79 p.

Federal Geodetic Control Committee, 1981, Specifications to support classification, standards of accuracy, and general specifications of geodetic control surveys: Nat. Oceanic and Atmospheric Admin., Rockville, Md, 46 p.

Fowkes, E. J., 1982, An educational guidebook to the geologic resources of the Coalinga district, California: Shannon Publications, Coalinga, 261 p.

Hart, E. W., and McJunkin, R. D., 1983, Surface faulting northwest of Coalinga, California, June and July 1983: This volume.

Harding, T. P., 1976, Tectonic significance and hydrocarbon trapping consequences of sequential folding synchronous with San Andreas faulting, San Joaquin Valley, California: American Assoc. Petrol. Geol. Bull., v. 60, p. 356-378.

Hartzell, S. H., and Heaton, T. H., 1983, Teleseismic mechanism of the May 2, 1983, Coalinga, California, earthquake from long period P-waves: This vol.

Holdahl, S. R., 1981, A model of temperature stratification for correction of leveling refraction: Bull. Geodesique, v. 55, p. 231-249.

_____, 1982, Recomputation of vertical crustal motions near Palmdale, California, 1959-1975: Jour. Geophys. Research, v. 87, p. 9374-9388.

Ireland, R. L., Poland, J. F., and Riley, F. S., 1982, Land subsidence in the San Joaquin Valley, California, as of 1980: U.S. Geol. Survey open-file report 82-370, 129 p.

Kanamori, H., 1983, Mechanism of the 1983 Coalinga earthquake determined from long period surface waves: This volume.

King, G. C. P., and Vita-Finzi, 1981, Active folding in the Algerian earthquake of 10 October 1980: Nature, v. 292, p. 22-26.

King, G., and Stein, R., 1983, Surface folding, river terrace deformation rate, and earthquake repeat time in a reverse faulting environment: The Coalinga, California, earthquake of May 1983: This volume.

Mansinha, L., and Smylie, D. E., 1971, The displacement fields on inclined faults: Seismol. Soc. America Bull., v. 61, p.1433-1440.

Mitten, H. T., 1972, Ground-water pumpage, San Joaquin Valley, California, 1967-68: U.S. Geol. Survey open-file report [not numbered], 6 p.

_____, 1976, Estimated ground-water pumpage in parts of the San Joaquin Valley, California, 1969-71: U.S. Geol. Survey open-file report, 7 p.

_____, 1980, Estimated agricultural ground-water pumpage in parts of the San Joaquin Valley, Califonia, 1975-77: U.S. Geol. Survey open-file report 80-1281, 11p.

Poland, J. F., Lofgren, B. E., and Ireland, R. L., 1975, Land subsidence in the San Joaquin Valley, California, as of 1972: U.S. Geol. Survey Prof. Paper 437-H, 78 p.

Prokopovitch, N. P., and Magelby, D. C., 1968, Land subsidence in Pleasant Valley: American Water Works Assoc. Jour., v. 60, p413-424.

Reasenberg, P., Eberhart-Phillips, D., and Segall, P., 1983, Preliminary views of the aftershock distribution, in Borcherdt, R. D., ed., The Coalinga earthquake sequence commencing May 2, 1983: U.S. Geol. Survey open-file report 83-511, 79 p.

Stein, R. S., 1981, Discrimination of tectonic displacement from slope-dependent errors in geodetic leveling from southern California 1953-1979, in Simpson, D. W., and Richards, P. G., eds., Earthquake Prediction, An International Review: Maurice Ewing Ser., v. 4, AGU, Wash., D.C., 680 p.

Stein, R. S., and Thatcher, W., 1981, Seismic and aseismic deformation associated with the 1952 Kern County, California, earthquake and relationship to the Quaternary history of the White Wolf fault: Jour. Geophys. Research, v. 86, p. 4913-4928.

Strange, W. E., 1980, The effect of systematic errors in geodynamic analysis, in Lachapelle, G., ed., 2nd Internat. Symp. on problems related to the redefinition of North American vertical geodetic network: Canadian Inst. Surveying, Ottawa, 978 p.

Wentworth, C. M., Walter, A. W., Bartow, J. A., and Zoback, M. D., 1983, The tectonic setting of the 1983 Coalinga earthquakes: Evidence from deep reflection and refraction profiles across the southeastern end of the Kettleman Hills: This volume.

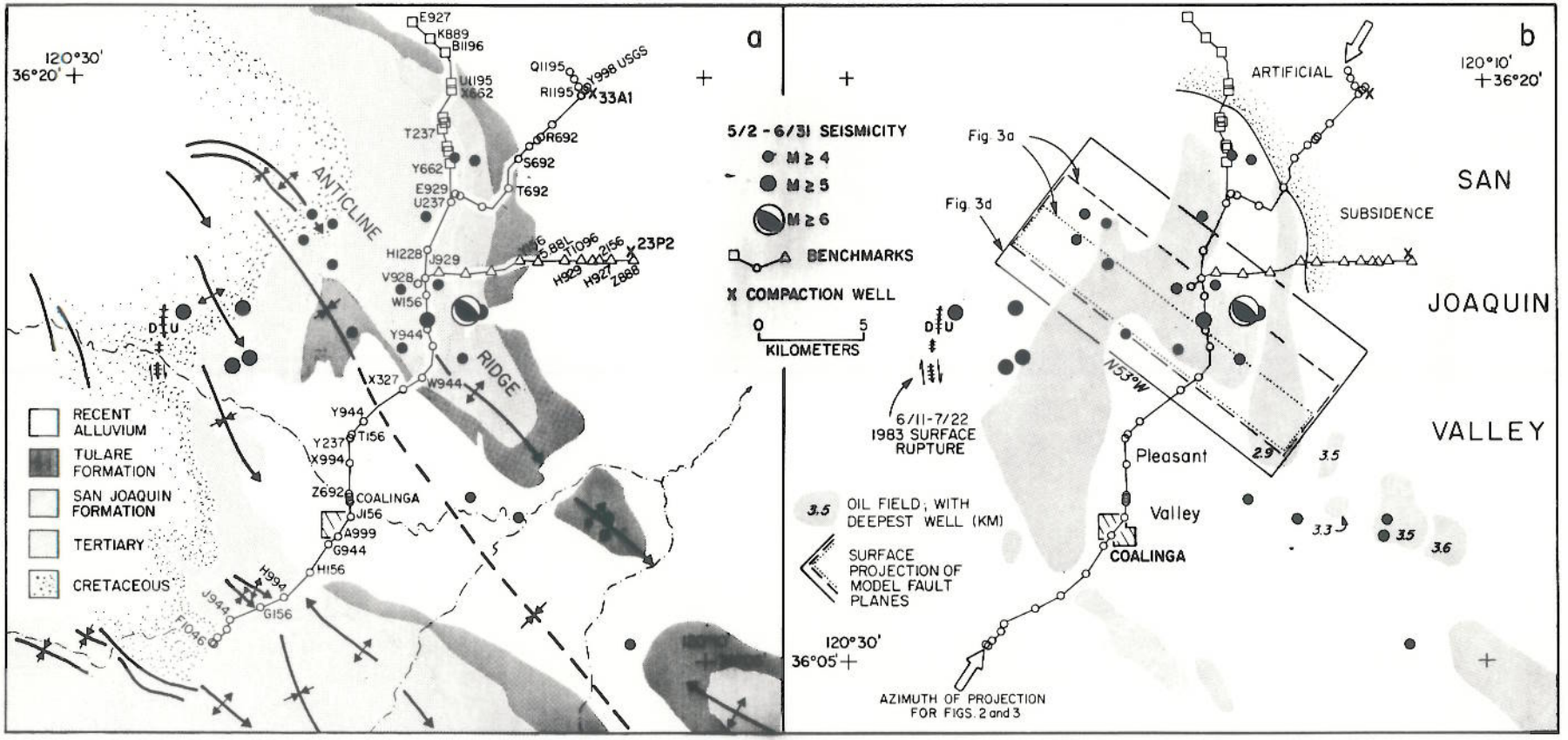

Figure 1. (a) Map of the leveling route, compaction recorder wells, geology, and structural features simplified from Fowkes (1982), with aftershocks. (b) Oil fields, showing the deepest well locations, the Nunez fault surface rupture, and the model fault planes projected to the ground surface.

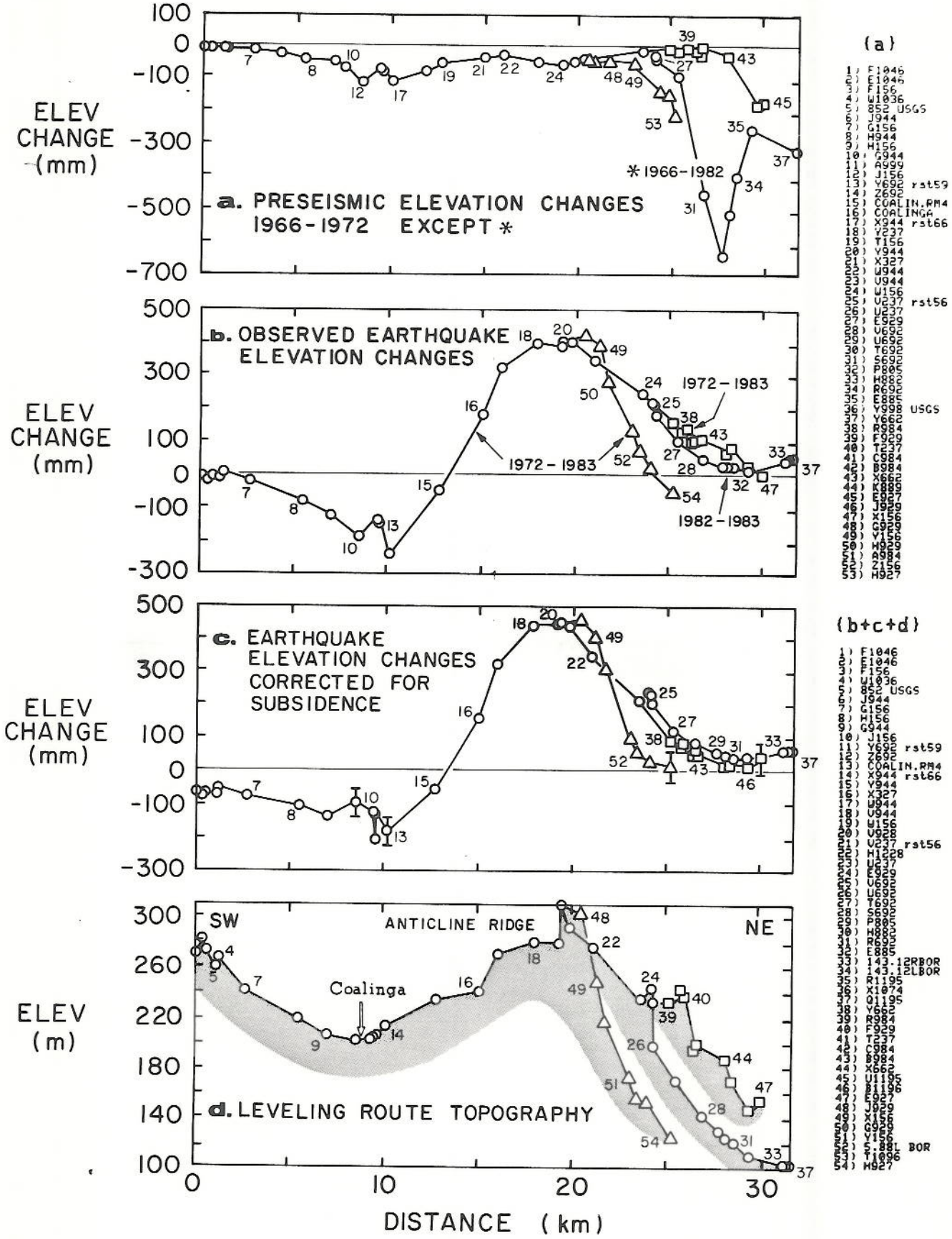

Figure 2. (a.-c.) Profiles of elevation change projected onto an azimuth N37°W, normal to the structural axis. Leveling errors are about equal to the size of the symbols; errors associated with the removal of artificial subsidence are shown by brackets in (c.). (d.) Leveling route topography.

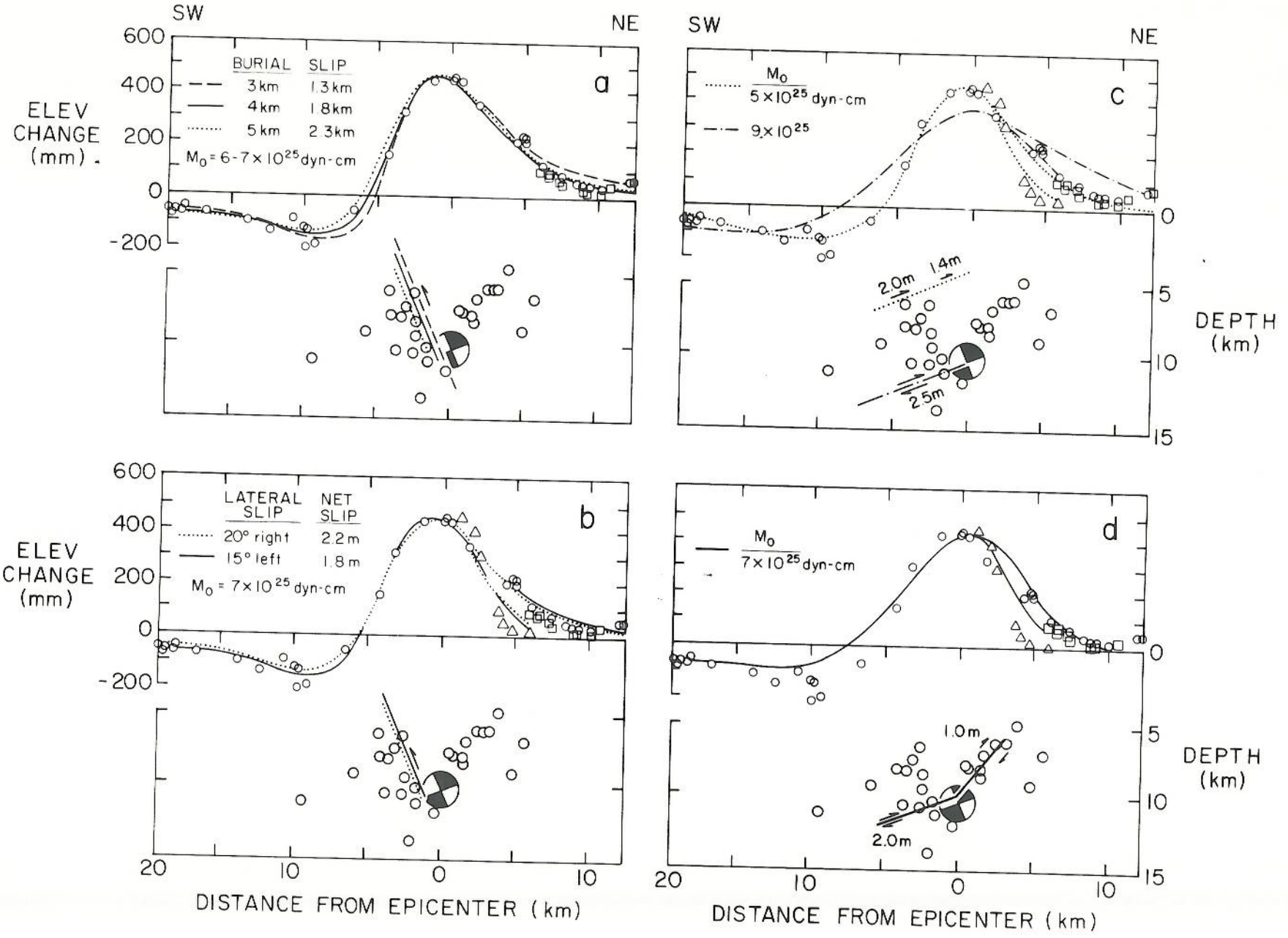

Figure 3. Earthquake elevation changes from Figure 2c compared with predicted deformation, together with a cross-section showing the model faults and the first four days of $M_L > 3$ aftershocks, and the mainshock. (a.-b.) Reverse faults with 67°NE dips. (c.-d.) Thrust faults dipping 23°SW.